SCIENTIFIC REPORTS
nature research

Check for updates

OPEN

Preparation and characterization of TiO_2 based on wood templates

Yu Liu[1], Xiaodong Zhu[2]✉, Diliang Yuan[1], Weicong Wang[1] & Lijiao Gao[1]

Titanium dioxide (TiO_2) was prepared from four natural wood spices that served as templates. The wood templates were impregnated by a titanium dioxide precursor and then underwent high-temperature calcination to obtain TiO_2 with a wood-like hierarchical porous structure. The microstructure of TiO_2 based on the wood template was characterized by scanning electron microscopy, X-ray diffraction and nitrogen adsorption–desorption tests. The formaldehyde adsorption and degradation properties of TiO_2 based on a wood template are discussed. The results showed that TiO_2 based on a wood template could effectively replicate the micro- and mesoscopic pore structure of wood, and the pore size distribution in the TiO_2 ranged from 1 to 100 nm. The TiO_2 that was prepared based on a wood template showed a certain adsorption effect on formaldehyde under visible light, and the photocatalytic degradation of a formaldehyde solution was achieved when irritated by ultraviolet light. In addition, the properties of the TiO_2 prepared by different tree species was also different. The TiO_2 prepared by larch and Chinese fir exhibited a large specific surface area, pore volume, and high degradation efficiency of formaldehyde solution. After 280 min of irradiation with an ultraviolet light source, the degradation rates of the formaldehyde solution were 19.91% and 18.85%.

In recent years, formaldehyde pollution of indoor air has been widely studied. The environmental protection and development of safety methods to deal with indoor formaldehyde and other decoration pollution has become a research hotspot[1–4]. The photocatalytic degradation of formaldehyde with TiO_2 has the advantages of energy savings, environmental protection, cleanliness and nontoxicity. It can degrade indoor pollutants and bacteria effectively[5–7].

The research and application of TiO_2 in the field of environmental protection have continuously increased[6,8–11]. Improving the catalytic activity of TiO_2 and preparing TiO_2 with an improved structure have become the main research directions. TiO_2 prepared by biological templates has important research and application value in terms of environmental protection and functional materials[12–15]. Using natural biomaterials as templates, the precursors of materials were impregnated into the templates by chemical or physical methods. Then, the templates were removed by calcination to obtain materials with natural biological morphology and structure[16]. The materials prepared by biological templates can effectively replicate the unique fine structure of organisms, optimize the structure and improve the performance.

Liu sintered TiO_2 with good catalytic effect by using butterfly wings and chloroplasts as biological templates[17]. Luo prepared TiO_2 materials with special properties and structures by using common filter paper as a template in the laboratory[18]. Li prepared TiO_2 with a leaf network structure by the biological template method[19]. Chen et Al. synthesized TiO_2 with a lignin template, and it exhibited a high photolytic activity[20]. Wood can also be used as a template to prepare certain oxides. The artificial Z-type reaction system of TiO_2 was prepared by five different wood templates. It was found that the hydrogen production of TiO_2 from wood templates was greatly improved by depositing precious metals[21]. Luo prepared TiO_2–wood charcoal composites by using wood as a template, and it showed extraordinary adsorption ability for BPA[22]. Li et al. fabricated C/SiC-ZrC composite ceramics from pine and oak wood and improved their compression strength[23].

As a natural biomass material, wood spices possess different microstructures. The preparation of a biomimetic TiO_2 material using wood as a template can improve the photocatalytic degradation efficiency by inheriting and optimizing the structure of the wood template, which is helpful for indoor air environment control. In this study, poplar, paulownia, Chinese fir and larch were selected as templates to prepare TiO_2. The effects of wood species on the photocatalytic degradation of formaldehyde and the microstructure of TiO_2 were investigated. The visible light degradation of TiO_2 based on wood templates was optimized by metal doping.

[1]College of Materials and Engineering, Northeast Forestry University, Harbin 150040, Heilongjiang, China. [2]Key Laboratory of Bio-Based Material Science and Technology (Ministry of Education), Northeast Forestry University, Harbin 150040, Heilongjiang, China. ✉email: pse4646@126.com

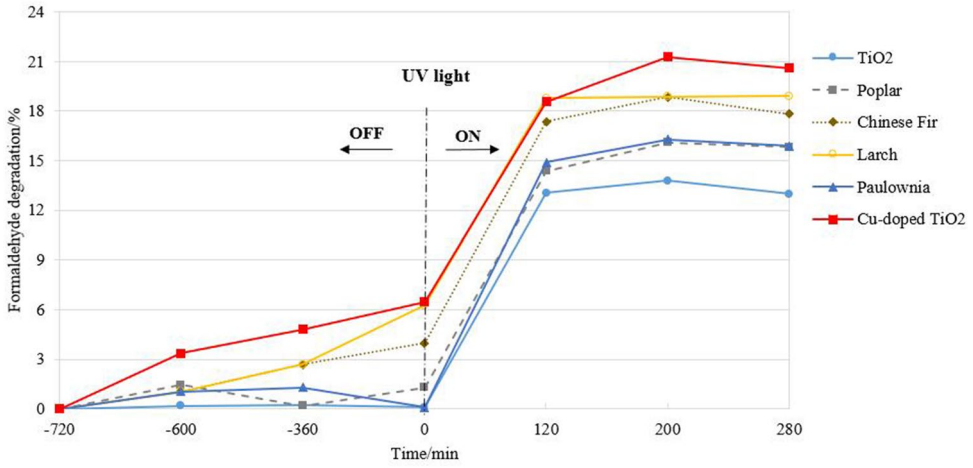

Figure 1. Degradation of the formaldehyde solution by different wood-templated TiO_2 before and after UV light irritation.

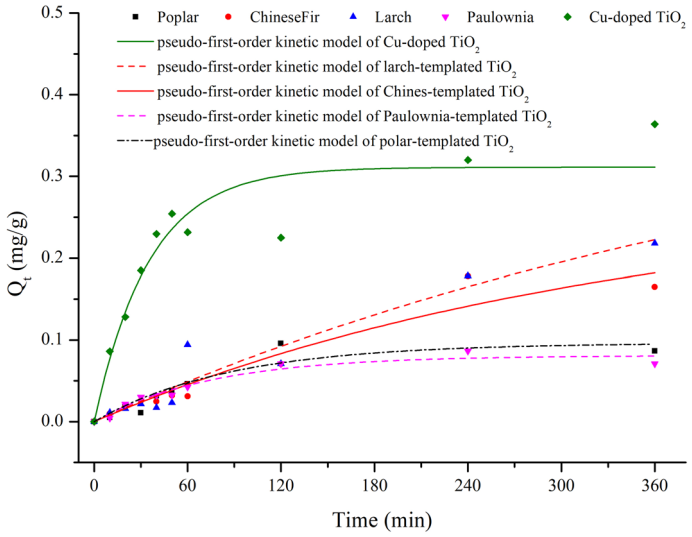

Figure 2. The adsorption kinetics curves of wood-templated TiO_2 on formaldehyde.

Results and discussion

Photocatalytic degradation of formaldehyde by TiO_2. Figure 1 shows the degradation of formaldehyde aqueous solution by TiO_2 under different light illumination conditions. Before turning on the ultraviolet light source, it was determined whether, or not, the four kinds of wood template TiO_2 need ultraviolet light to stimulate electrons to produce photodegradation. Therefore, the TiO_2 adsorbed formaldehyde in solution first. Among the four types of wood templates, TiO_2 prepared from larch and Chinese fir showed an improved adsorption of formaldehyde solution without ultraviolet (UV) light.

The effects of the four types of TiO_2 prepared with poplar, Paulownia, Chinese fir and larch templates on the formaldehyde concentration showed no significant difference during the first 2 h. However, the concentration of formaldehyde solution treated with TiO_2 prepared with larch and Chinese fir templates decreased after 6 h, and this trend continued to increase as the standing time increased. The concentration of the formaldehyde solution with larch and Chinese fir-templated TiO_2 decreased by 6.27% and 3.97%, respectively, at 12 h. However, formaldehyde desorption occurred in the solution with poplar- and Paulownia-templated TiO_2 during static processing, which made the concentration of formaldehyde solution fluctuate significantly.

To better understand adsorption phenomena, adsorption kinetics were also examined. As Fig. 2 and Table 1 showed, the adsorption followed pseudo-first-order kinetics, which is directly proportional to the dose. Cu-doped poplar-templated TiO_2 showed the highest adsorption rate, followed by the hardwood-templated TiO_2.

The catalytic degradation of formaldehyde in aqueous solution with copper-doped TiO_2 occurred under visible light. Figure 1 shows that the concentration of formaldehyde solution treated with copper-doped poplar-templated TiO_2 declined continuously within 12 h, and the highest degradation rate reached 6.48%. This was

Type of TiO_2	Qe,exp (mg g^{-1})	k_1 (min^{-1})	Qe,cal (mg g^{-1})	R^2
Poplar-templated TiO_2	0.0865	0.0114	0.0964	0.88
Chinese fir-templated TiO_2	0.1648	0.0030	0.2751	0.94
Larch-templated TiO_2	0.2180	0.0020	0.4366	0.93
Paulownia-templated TiO_2	0.0709	0.0133	0.0810	0.95
Cu-doped poplar-templated TiO_2	0.3639	0.0283	0.3112	0.89

Table 1. Kinetic parameters obtained from the pseudo-first-order models of formaldehyde adsorption onto TiO_2.

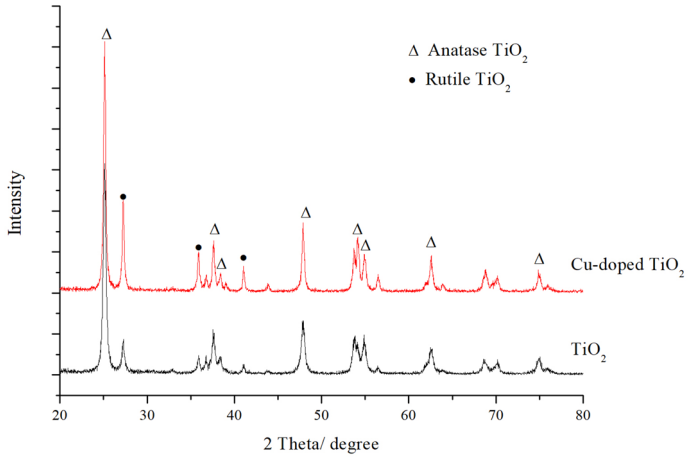

Figure 3. XRD analysis of TiO_2 prepared with poplar template.

related to the increasing utilization of solar light by the copper-doped poplar-templated TiO_2 and the broadening of the response wavelength of the TiO_2. The doping of copper ions increased the utilization of solar light and broadened the response wavelength of the TiO_2 prepared with the wood templates.

When the ultraviolet light turned on, four types of TiO_2 showed an aldehyde-reducing effect on the formaldehyde aqueous solution. As shown in Fig. 1, the degradation of formaldehyde by the TiO_2 prepared with the wood templates increased with an extension of the ultraviolet irradiation time, but the degradation efficiency was slightly different under the same illumination intensity. The concentration of formaldehyde solution treated with TiO_2 prepared without a wood template decreased 13.05% after 2 h of ultraviolet light irritation. The maximum degradation efficiency of the formaldehyde solution was 13.8% within 280 min of irradiation. The degradation of the formaldehyde aqueous solution treated with wood-templated TiO_2 under ultraviolet light was better than that of the formaldehyde solution without templated titanium dioxide. Copper-doped wood-templated TiO_2 showed the highest degradation efficiency of 21.62%. The larch- and Chinese fir-templated TiO_2 also exhibited improved degradation effects on the formaldehyde solution with degradation rates of 19.91% and 18.85%, respectively. To compare the UV degradation efficiency of all samples, the experimental data for the photocatalytic degradation of the formaldehyde aqueous solution by titanium dioxide with and without templates were integrated, and the reaction rate constant was calculated. The results showed that the apparent first-order rate constants for titanium dioxide without a template and poplar-templated TiO_2, Chinese fir-templated TiO_2, larch-templated TiO_2, Paulownia-templated TiO_2 and Cu-doped poplar-templated TiO_2 were 0.0006, 0.0008, 0.0009, 0.0009, 0.0008 and 0.001, respectively. The TiO_2 duplicated the microporous structure in the wood template and showed a stronger ultraviolet absorption ability. It absorbed an increased excitation energy to excite electrons, which is conducive to the photodegradation of titanium dioxide. The factors affecting the photocatalytic effect include the size, specific surface area and porosity of TiO_2 grains. A smaller grain size and larger specific surface area increase the chance of contact between the particle surface and organic matter, which is conducive to the improvement of photocatalytic activity. This has been verified in the subsequent analysis of the microstructure characterization of the larch- and Chinese fir-templated TiO_2.

XRD. Figure 3 shows the X-ray diffraction (XRD) patterns of the poplar-templated TiO_2 and copper-doped poplar-templated TiO_2. Most of the TiO_2 formed by calcination of the wood at 600 degrees comprised the anatase phase, and a minor amount comprised the rutile phase. According to the calculation, the average grain size of the poplar-templated TiO_2 was 18.8 nm, and the crystallinity was 61.82%. The copper doping had no significant effect on the crystalline form of the TiO_2 from the wood template, and its diffraction peaks were mainly anatase and rutile, which were the same as those from the TiO_2 from the undoped wood template. After copper

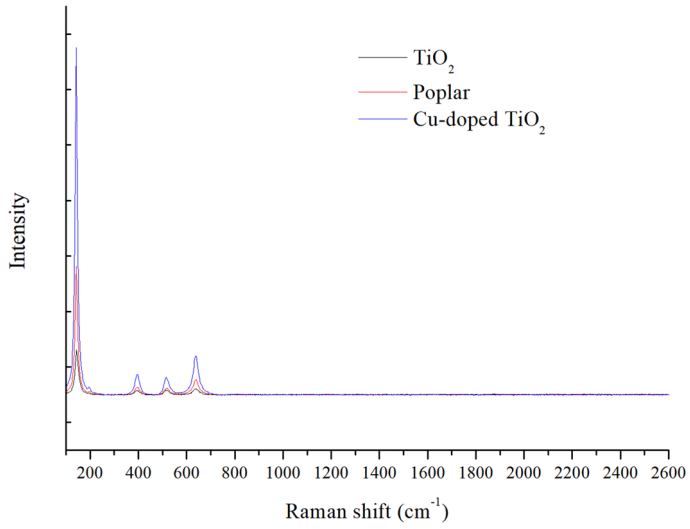

Figure 4. Raman spectra of TiO_2.

doping, the intensity of the main characteristic diffraction peaks from the TiO_2 in the wood template increased as the crystallinity increased. The width of the peaks narrowed slightly, and the average grain size increased to 28.1 nm. The characteristic diffraction peak area of the TiO_2 rutile-type copper-doped wood template obviously increased, and the content increased. It may be that the doping of copper reduced the phase transition temperature of the anatase, which increased the structure of the TiO_2 rutile type of copper-doped wood template after the same calcination process. At the same time, there were no obvious characteristic peaks of copper-containing substances in the XRD patterns, which was related to the small amount of copper doping and the fact that copper doping does not form an independent phase but enters the crystal structure[24].

Raman spectroscopy analysis. Raman spectroscopy was used to study the internal structure of the catalyst. Figure 4 shows the Raman spectra of the TiO_2 photocatalyst with and without a wood template and the Cu-doped wood-templated TiO_2. In the figure, the peaks at 145 cm^{-1}, 422 cm^{-1}, 515 cm^{-1} and 639 cm^{-1} belong to the anatase phase of TiO_2, while the peak at 216 cm^{-1} belongs to the rutile phase of TiO_2. Because the lattice vibration of rutile is weaker than that of anatase, the other Raman characteristic peaks of rutile were covered by the anatase phase. It can be seen from the figure that the strongest anatase Raman peaks at approximately 145 cm^{-1} increased with the use of wood templates. The lattice vibration of the noble metal Cu was not measured for the same reasons diffraction peaks were not measured by XRD. The half width of the Raman peak at 145 cm^{-1} increased with increasing Cu doping. In addition, as the Cu loading of the noble metal increased, the position of the Raman peak of TiO_2 redshifted, and the intensity of the peak gradually strengthened.

SEM and TEM. The microscopic morphology of wood-templated TiO_2 was observed by scanning electron microscopy (SEM). The results are shown in Fig. 5. In the images of the Paulownia-templated TiO_2, 50 μm macropores can be observed, which were mainly inherited from the Paulownia wood. At the same time, in the longitudinal section of the poplar, Chinese fir, larch and Paulownia, 10–20 μm cellular fibrous pores can also be observed, and the pore structure below 5 μm on the cell wall was duplicated. Pits are the main pathway for water transfer between cells in wood. In this study, the original pit plugs and pit membranes in the pits were partially removed through hydrothermal pretreatment, which enabled the TiO_2 precursor to enter the pores of the wood cells and replicate the micropore structure of the wood effectively during sintering. During the precursor impregnation process, the precursor solution was evenly adsorbed or precipitated in the wood cell walls instead of accumulating in the pores in two ways: osmotic flow and diffusion. The transformation of the residual structure was achieved by optimizing the ratio of precursor solution and impregnation conditions. During the calcination stage, the precursor adsorbed on the cell wall was directly oxidized to produce the corresponding metal oxide phase, and at the same time, the original wood component was removed, and the porous structure of the wood was inherited from the oxide phase. The existence of a macropore structure is conducive to the improvement of photocatalytic performance, which is mainly because it provides a uniform and rapid diffusion channel for the adsorbed gas to the inside of the material, greatly increasing the reaction area with the measured gas.

The color of the copper-doped wood-templated TiO_2 was lavender red, while the undoped TiO_2 in the wood template was a white powder, as shown in Fig. 6. The EDS results show that the preparation of wood-templated TiO_2 with the method described in the experiment section removed the template material while retaining the microstructure of the wood template. Only Ti and O elements were detected in the sample. The copper doping process can indeed dope copper into the TiO_2 of the wood template. However, the content was low mainly due to the small amount of doping. At the same time, the morphology of TiO_2 doped with copper retained the fine

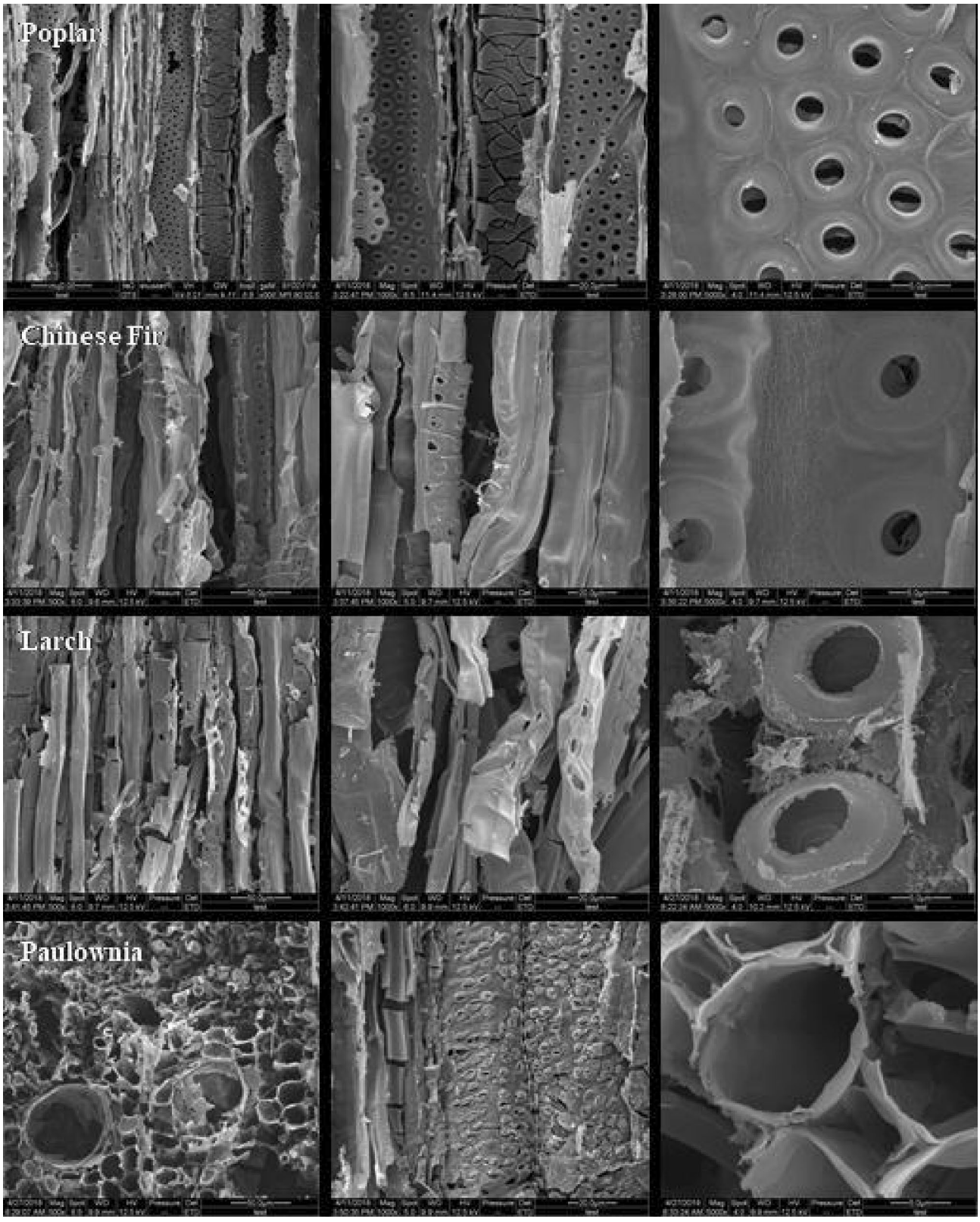

Figure 5. SEM images of wood-templated TiO_2.

structure of the wood. Copper, Ti and O together constituted the pore wall part of the product structure, while the original C in the wood structure was completely removed by high-temperature oxidation calcination.

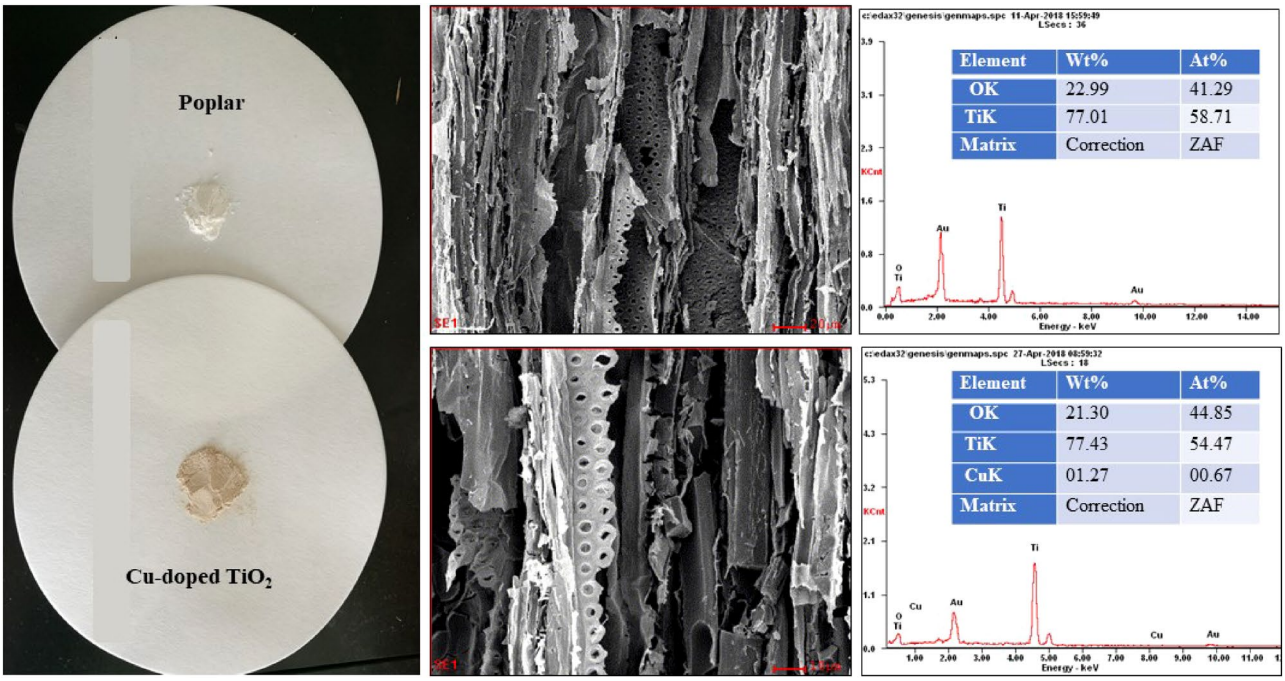

Figure 6. EDS analysis of the TiO_2 prepared with the poplar template.

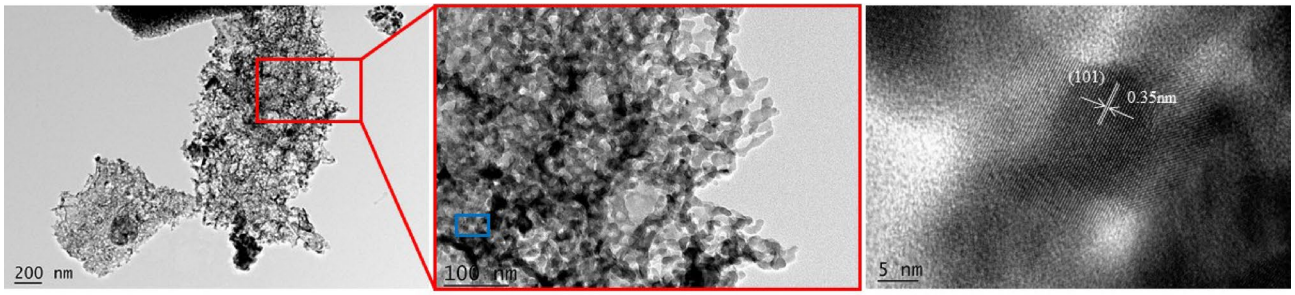

Figure 7. TEM analysis of TiO_2 prepared with the poplar template.

In Fig. 7, the calcination products retained pit structure of wood. TiO_2 particles were well crystallized and appear as crystalline hexagonal shape with sizes of 15–30 nm. A typical HRTEM image of the sphere wall as marked by a blue box was displayed in Fig. 7, in which a crystal lattice fringe with the spacing d value of 0.35 nm corresponds to the (101) crystal facets of TiO_2 anatase type.

Pore size and structure. Figure 8 shows the nitrogen adsorption–desorption isotherms and pore size distribution of TiO_2 synthesized with different types of wood templates. The nitrogen adsorption–desorption isotherm curve of the wood-templated TiO_2 synthesized in this experiment is a typical type IV curve with an H3 hysteresis ring, which indicates that the synthesized TiO_2 had a mesoporous structure. Moreover, there was a sharp jump at the relative pressure P/P = 0.8–1.0, which was caused by capillary condensation. At the same time, the ring cannot be closed at low pressure, which indicates that the material contained an irregular nanoporous structure. The results show that the pore size distribution of the wood-templated TiO_2 was relatively wide.

The specific surface area, pore volume and pore size of the TiO_2 were calculated with the adsorption isothermal data, as shown in Table 2. The specific surface area and pore volume of soft woods Chinese fir and larch were larger than those of hard woods Paulownia and poplar. The specific surface area of the Chinese fir was the largest, reaching 19.3991 m^2/g. The TiO_2 from the Paulownia template had the largest average pore size, followed by larch, poplar and Chinese fir. Different specific surface areas and pore sizes directly affected the microstructure of the wood-templated titanium dioxide.

At present, there are some reports on the synthesis of TiO_2 using fiber templates to produce a porous material for photocatalysis degradation. In particular, the modification of TiO_2 with nature plant fibers were found to improve the adsorption capacity, and it provide more efficiency for metal particles assembling on the nanopores. Different microstructures of TiO_2 had a certain selectivity for the target degradation products. Compared with metallic oxide synthesized from other fiber template, such as rice husk, cotton fiber, tree leave, the size and shape of pore structure of wood templated TiO_2 can be adjusted by choosing the appropriate wood species. An

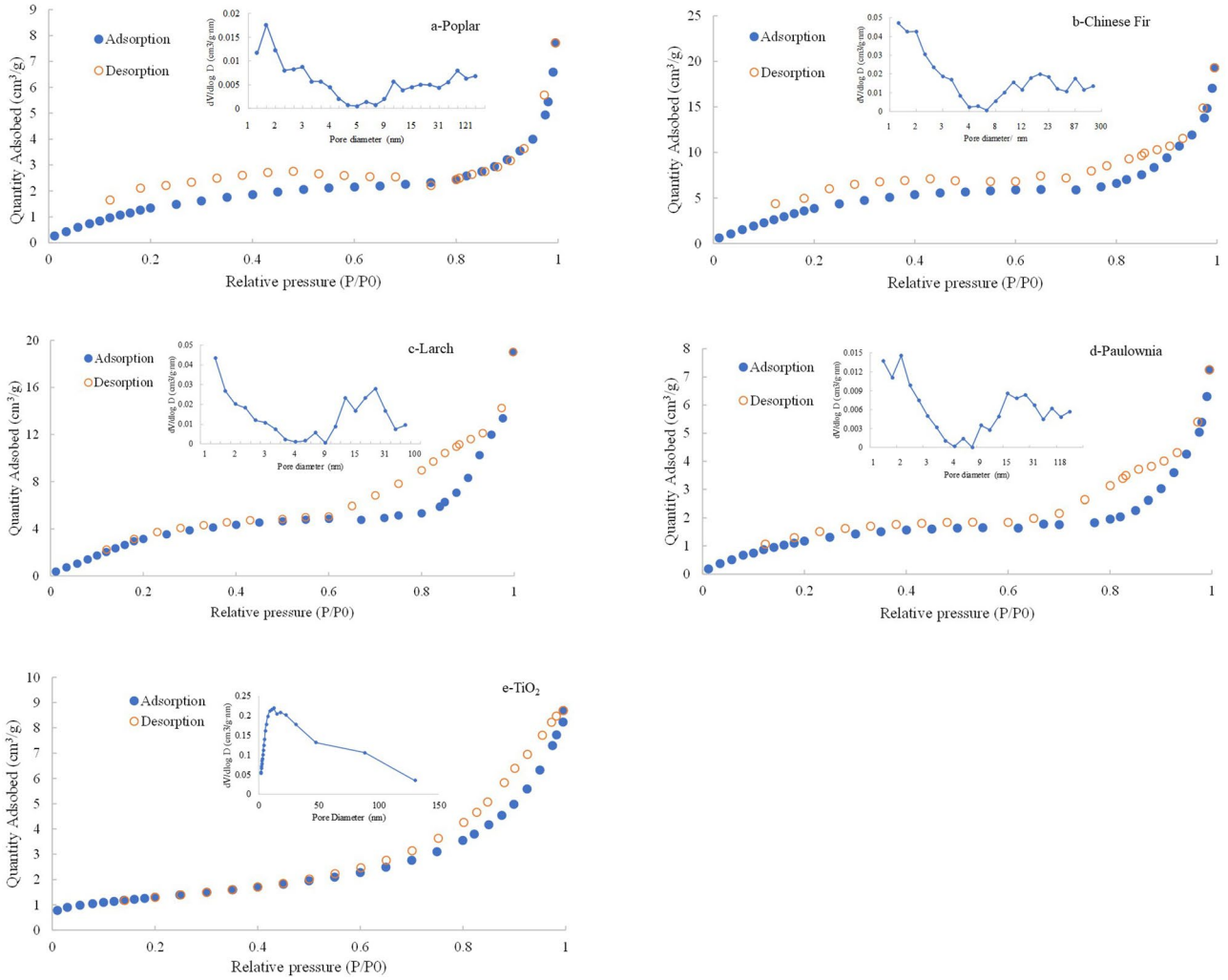

Figure 8. N_2 adsorption/desorption isotherms of TiO_2 prepared with different wood templates.

Samples	BET (m^2/g)	Pore volume (cm^3/g)	Adsorption average pore diameter (nm)	Desorption average pore diameter (nm)
Poplar	6.1109	0.0111	8.0548	12.8337
Chinese fir	19.3991	0.0272	6.8251	9.0057
Larch	17.5101	0.0283	8.9026	8.3464
Paulownia	5.3828	0.0107	9.2249	10.1131
TiO_2 without a template	104.64	0.2530	9.9796	9.4455

Table 2. N_2 adsorption measurement data for the wood-templated TiO_2.

appropriate pore size was conducive to the transport and reaction of target degradation products into the active regions of the TiO_2 in the wood template, which then produced different catalytic effects.

UV–Vis spectroscopy. Figures 9 and 10 show the UV–Vis DRS spectra for the different samples. Curve (a) is the UV–Vis spectrum of TiO_2. It can be seen that the band gap width of the TiO_2 was 3.2 eV, which demonstrated strong absorption in the UV region (in < 400 nm), but there was almost no absorption in the visible region. This indicated that light with a wavelength of 400 nm was not absorbed and utilized, so the energy contained in the photon in the visible region did not excite the electron transition from the valence band to the conduction band; (b) and (c) are the UV–Vis spectra of the wood-templated TiO_2. It can be seen from the spectra that the absorption of ultraviolet light by the wood-templated titanium dioxide decreased, but the absorption in the visible light region increased. The wavelength of the absorption edge of the wood template redshifted, and the width of the band gap decreased.

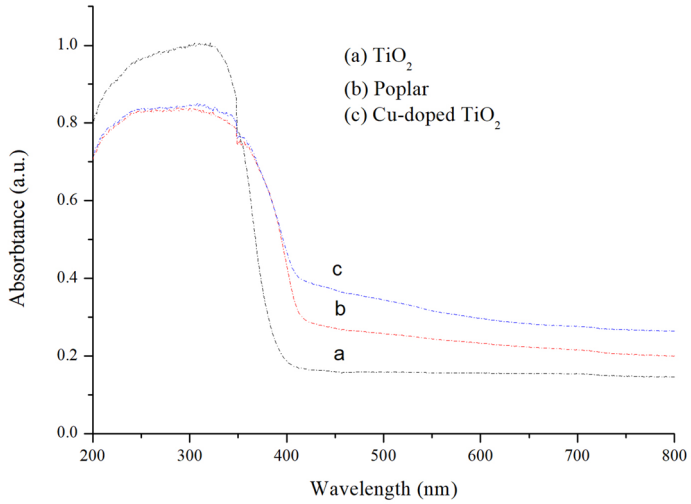

Figure 9. UV–Vis absorption spectra for TiO_2.

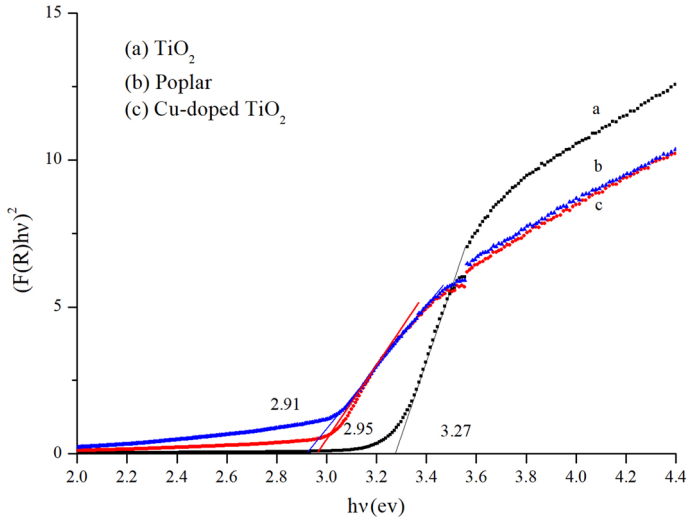

Figure 10. Plot of $F(R)hv^2$ versus photon energy for TiO_2.

Conclusions

Wood treated by hydrothermal extraction was adopted for TiO_2 preparation, and porous TiO_2 with a wood-like microstructure was formed after high-temperature calcining. The TiO_2 obtained by this method successfully reproduced the microporous and mesoporous structure of the wood. The wide pore size distribution ranged from 1 to 100 nm. The results show that the pore structure parameters of the TiO_2 were related to the wood species. For the same preparation process, the specific surface area and pore volume of the TiO_2 obtained from the larch and Chinese fir templates were higher than those obtained from the poplar and Paulownia templates. The crystal structure of the obtained TiO_2 was a mixture of anatase phase and rutile phase. In the photocatalytic degradation testing of the formaldehyde aqueous solution, the TiO_2 with a porous wood structure showed better absorption and utilization of light than the ordinary titanium dioxide. The formaldehyde degradation efficiency of copper-doped poplar-templated TiO_2 reached 21.62% in 280 min.

Methods

Materials. The poplar (air-dry density 0.48 g/cm^3), Paulownia (air-dry density 0.32 g/cm^3), Chinese fir (air-dry density 0.47 g/cm^3), and larch (air-dry density 0.40 g/cm^3) were provided by Heilongjiang Yabuli Wood Industry Co., Ltd. The moisture content of the wood specimen was 4%. The butyl titanate, glacial acetic acid, acetylacetone and ammonium acetate were purchased from the Tianjin Guangfu Fine Chemical Research Institute.

Preparation of TiO_2 from the wood templates. To remove the extractives from the wood and open channels to transport the TiO_2 precursor into the wood, hydrothermal treatment of the wood template was carried out. The poplar, Paulownia, Chinese fir and larch were sawed into small blocks with a size of $20 \times 20 \times 2$ mm. Samples without nodules and decay defects were selected and treated in a hot water bath at 50 °C for 3 h. The samples were dried in a constant temperature drying oven at 60 °C for 6 h and then dehydrated with anhydrous ethanol. The precursor impregnating solution was prepared with butyl titanate, absolute ethanol, deionized water and glacial acetic acid in a molar ratio of 1:9:3:2. The butyl titanate was mixed with 2/3 volume of absolute ethanol to form liquid A, and 1/3 volume of absolute ethanol was mixed with deionized water and glacial acetic acid to form liquid B. The dewatered wood was impregnated in liquid A for 4 h, liquid B was dripped slowly into liquid A within 15 min, and then, the wood templates were taken out to air dry for 12 h under room conditions. Finally, the treated wood samples were put into a tubular furnace for high-temperature calcination. During the heating process, the temperature was slowly raised from room temperature to 260 °C and held for 40 min, then the temperature increased from 260 to 600 °C for 180 min.

Preparation of copper-doped TiO_2. To improve the visible light photocatalytic properties of the TiO_2, the precursor solution was prepared with a molar ratio of butyl titanate: deionized water: absolute ethanol: glacial acetic acid: copper acetate = 1:3:9:2:0.0015. The specific operation methods were as follows: (1) butyl titanate was mixed with 2/3 of anhydrous ethanol to form liquid A; (2) the remaining 1/3 of anhydrous ethanol was mixed with glacial acetic acid to form liquid B; (3) copper acetate was dissolved in deionized water, stirred and dissolved to form liquid C; and (4) liquid C was added into liquid B, fully stirred and mixed to form liquid D. The wood treated by the hydrothermal pretreatment was put into liquid A. After being impregnated for 4 h under ultrasonic conditions, liquid D was slowly dripped into liquid A and reacted for 15 min. After the reaction, the wood samples were removed and air-dried for 12 h at room temperature. The copper-doped wood-templated TiO_2 was prepared by calcination in a high-temperature tubular furnace.

Photocatalytic degradation of the formaldehyde. In this study, a certain quantity of wood-templated TiO_2 was put into the formaldehyde aqueous solution with a concentration of 10 mg/l. After mixing uniformly, the solution was irradiated by different light sources. The concentration of the formaldehyde solution after irritation was determined by spectrophotometry to investigate the TiO_2 photocatalytic degradation of the formaldehyde solution.

Characterization. The crystal structure of TiO_2 from the wood template was characterized by XRD. Scanning electron microscopy (SEM) and EDS were used to observe the structure of the wood-templated TiO_2. At the same time, nitrogen adsorption–desorption tests were carried out to measure the specific surface area, pore size and distribution of the samples. The pore structure replication of TiO_2 from the wood template was also analyzed.

Received: 2 July 2019; Accepted: 9 July 2020
Published online: 24 July 2020

References

1. Tang, Z., Zhan, X., Yang, Y., Yan, W. & Xu, X. Impregnation process and properties of thin veneers with melamine formaldehyde resin. *J. For. Eng.* **3**, 32–37 (2018).
2. Wang, W., Liu, Y. & Zhu, X. Control of formaldehyde release of surface veneered panels based on urea microcapsule. *J. For. Eng.* **3**, 38–42 (2018).
3. Zhang, Z., Guan, M. & Liu, Y. Degradability of bamboo shoot shell/UF modified starch adhesive composites. *J. Nanjing For. Univ. (Nat. Sci. Ed.)* **41**, 160–166 (2017).
4. Yuan, B., Dong, Y. & Guo, M. Immobilized of g-C3N4 on wood surface and characterization of its photodegradation property. *J. Nanjing For. Univ. (Nat. Sci. Ed.)* **42**, 193–197 (2018).
5. Shayegan, Z., Haghighat, F. & Lee, C.-S. Photocatalytic oxidation of volatile organic compounds for indoor environment applications: three different scaled setups. *Chem. Eng. J.* **357**, 533–546 (2019).
6. Chen, A. *et al.* Enhanced sunlight photocatalytic activity of porous TiO2 hierarchical nanosheets derived from petal template. *Powder Technol.* **249**, 71–76 (2013).
7. Paolini, R., Borroni, D., Pedeferri, M. & Diamanti, M. V. Self-cleaning building materials: the multifaceted effects of titanium dioxide. *Constr. Build. Mater.* **182**, 126–133 (2018).
8. Liu, R. F., Li, W. B. & Peng, A. Y. A facile preparation of TiO2/ACF with C Ti bond and abundant hydroxyls and its enhanced photocatalytic activity for formaldehyde removal. *Appl. Surf. Sci.* **427**, 608–616 (2018).
9. Qi, L., Cheng, B., Yu, J. & Ho, W. High-surface area mesoporous Pt/TiO(2) hollow chains for efficient formaldehyde decomposition at ambient temperature. *J. Hazard. Mater.* **301**, 522–530 (2016).
10. Li, X.-S. *et al.* Plasma-promoted Au/TiO2 nanocatalysts for photocatalytic formaldehyde oxidation under visible-light irradiation. *Catal. Today* **337**, 132–138 (2019).
11. Ceylan, H. *et al.* Size-controlled conformal nanofabrication of biotemplated three-dimensional TiO2 and ZnO nanonetworks. *Sci. Rep.* **3**, 2306 (2013).
12. Chen, J. Y., Yang, C. Y. & Chen, P. Y. Synthesis of hierarchically porous structured CaCO3 and TiO2 replicas by sol–gel method using lotus root as template. *Mater. Sci. Eng. C Mater. Biol. Appl.* **67**, 85–97 (2016).
13. Chen, Z. *et al.* Preparation of porous TiO2 using eggshell membrane as template and its photocatalytic activity. *Procedia Eng.* **27**, 512–518 (2012).
14. Hui, C., Lei, Z., Xitang, W., Shujing, L. & Zhongxing, L. Preparation of nanoporous TiO2/SiO2 composite with rice husk as template and its photocatalytic property. *Rare Met. Mater. Eng.* **44**, 1607–1611 (2015).
15. Munafò, P., Goffredo, G. B. & Quagliarini, E. TiO2-based nanocoatings for preserving architectural stone surfaces: an overview. *Constr. Build. Mater.* **84**, 201–218 (2015).

16. Tang, Y. *et al.* Electrochemical aptasensor based on a novel flower-like TiO2 nanocomposite for the detection of tetracycline. *Sensors Actuators B Chem.* **258**, 906–912 (2018).
17. Liu, X. *Sonochemical Synthesis of Morphogenetic Materials and Investigation of Its Optic Properties*. Master thesis, Shanghai Jiao Tong University (2011).
18. Luo, Y. *Fabrication and Application of Hierarchical Titania-Containing Nanocomposite Materials Based on Natural Cellulose Substance*. Doctor thesis, Zhejiang University (2015).
19. Li, J., Li, Q., Zhao, J. & Li, B. Preparation and photocatalytic properties of reticular TiO2 by leaf template method. *Acta Chim. Sin.* **68**, 1845–1849 (2010).
20. Chen, X., Kuo, D.-H., Lu, D., Hou, Y. & Kuo, Y.-R. Synthesis and photocatalytic activity of mesoporous TiO2 nanoparticle using biological renewable resource of un-modified lignin as a template. *Microporous Mesoporous Mater.* **223**, 145–151 (2016).
21. Pan, J. *Artificial Z-Scheme Photocatalytic System Based on Wood-Templated TiO2*. Master thesis, Shanghai Jiao Tong University (2013).
22. Luo, L. *et al.* A novel biotemplated synthesis of TiO2 /wood charcoal composites for synergistic removal of bisphenol A by adsorption and photocatalytic degradation. *Chem. Eng. J.* **262**, 1275–1283 (2015).
23. Li, J. *et al.* Fabrication and characterization of biomorphic cellular C/SiC–ZrC composite ceramics from wood. *Ceram. Int.* **41**, 7853–7859 (2015).
24. Bu, D. & Zhuang, H. Biotemplated synthesis of high specific surface area copper-doped hollow spherical titania and its photocatalytic research for degradating chlorotetracycline. *Appl. Surf. Sci.* **265**, 677–685 (2013).

Acknowledgements

This work was supported by the fundamental research funds for the central universities (2572017CB21), Heilongjiang Natural Science Foundation (C2017002)

Author contributions

Y.L. conceived and designed the experiments; W.W. performed the experiments; D.Y. conducted a supplementary experiment; L.G. analyzed the data; and Y.L. and X.Z. wrote the paper.

Competing interests

The authors declare no competing interests.

Additional information

Correspondence and requests for materials should be addressed to X.Z.

Reprints and permissions information is available at www.nature.com/reprints.

Publisher's note Springer Nature remains neutral with regard to jurisdictional claims in published maps and institutional affiliations.